Delft University of Technology

Market-orientated solutions to increase thermal conductivity in latent thermal energy storage systems

Righetti, Giulia; Zilio, Claudio; Hooman, Kamel; Mancin, Simone

Important note
To cite this publication, please use the final published version (if applicable).
Please check the document version above.

Research Paper

Market-orientated solutions to increase thermal conductivity in latent thermal energy storage systems

Giulia Righetti [a,*], Claudio Zilio [a], Kamel Hooman [b], Simone Mancin [a]

[a] *Department of Management and Engineering, University of Padova, Vicenza, Italy*
[b] *Process and Energy Department, Delft University of Technology, the Netherlands*

ABSTRACT

Among experts, it is well-known that the thermal conductivity of PCMs (phase change materials) is low hence a major limitation for their commercial application. This work proposes alternative, inexpensive, but nevertheless effective solutions to increase the average thermal conductivity of a PCM system (a commercial paraffin wax, having a phase change temperature of about 40 °C) used for thermal energy storage. 600 g of PCM fills an annulus wrapping an inner tube used to either charge or discharge heat to the PCM. The effect of the flow rate and temperature of the water used as heat transfer fluid was experimentally analysed. The flow rate was set to vary between 2 and 8 l min⁻¹ and the temperature between 45 and 55 °C. We tested three different aluminum-based thermal enhancers: a commercially available metal foam sample, a wire mesh, and irregular flakes (chips) obtained as waste product of machining operations. The PCM-only sample exhibited the longest charging and discharging times, while the PCM + foam sample shortened them the most. The two cost-effective solutions (chip and wire mesh) resulted in intermediate phase change times. A performance indicator, in terms of cost per phase change rate, is proposed to compare different enhancers. It demonstrated that these two cost-effective thermal conductivity enhancing solutions can become a key enabling method to widely deploy latent thermal energy technology widely in many different applications.

1. Introduction

Phase Change Material (PCM) is a material that is capable of storing latent energy during its solid to liquid phase transition, thus offering the possibility of storing a large amount of heat in small volumes over a very narrow temperature range [1]. Therefore, PCMs can decouple energy production from energy consumption. Latent Thermal Energy Storages (LTES) based on PCMs can store the surplus of energy produced by plants/systems that work discontinuously, as is the case with most of renewable energy sources.

PCMs are now commercially available, but many of them suffer from low thermal conductivity, which varies in the range between 0.1 and $0.3 \text{ W m}^{-1} \text{ K}^{-1}$ for organic ones, leading to slow charge and discharge as well as non-uniform temperature distribution in the storage tank [1]. This penalization of heat transfer is a major limitation hindering the application of PCMs as thermal storage systems. Hence, a great deal of information is available in the literature on this very topic. Most often the solution is offered through the addition of highly-conductive materials (metals). For example; fins and inserts of various shapes, porous

materials, or nanoparticles (see the review papers by [2–5] and the chapter by Mancin in [1]). Among these options, metal foams stand out thanks to their very high equivalent thermal conductivity leading to a fast and uniform phase change process.

For instance, Heyhat et al. [6] compared metal foam, fin, and nanoparticles to improve the performance of a PCM-based passive thermal management system of a lithium-ion battery. The authors observed that the addition of nanoparticles had an insignificant effect on thermal management, fins did not always lead to system improvement, while foam was the most effective way to reduce the mean temperature and improve the performance.

Nonetheless, the cost of foams is too high to make them a competitor in large scale applications [7].

In an attempt to minimise the cost, Liu et al. offered a hybrid solution as a copper fin-foam compound. According to those authors, the hybrid system works even better than the original metal foam. However, brazing the foam to fins over extended surface area adding significantly to the cost of the compound.

Less expensive options, including fins and metal meshes/matrices, are investigated in the literature with performance closing in on metal

temperature distribution and a shorter time to achieve thermal equilibrium. A maximum improvement of 24 % was observed compared to the pure PCM option.

Zhao et al. [11] and Opolot et al. [12] immersed a commercial SS-304 mesh in a PCM-filled annulus, wrapped around an air (HTF) tube. The system was charged using an electrical heater and discharged with cold air to represent PCM storage for high-temperature (~700 °C) heat storage. Implementing the periodic structure showed superior performance in terms of heat transfer enhancement, reducing the melting time by 19.4 % and the overall cycle by about 10 % compared with that of pure PCM.

Ganji et al. [13] optimised the volume of metal mesh within a PCM enclosure. According to those authors, a full-coverage wire mesh limits natural convection while covering only 62.5 % of the total tank height reduces the charging time by 34 %.

Zhao et al. [14] have offered recommendation to design a PCM storage tank with fin/wire inserts. According to those authors, the optimal enhanced height depends on a number of parameters including the Rayleigh number and fin/PCM thermal conductivity ratio.

In view of the above, there exists a trade-off between performance and cost for PCM-based thermal energy storage and/or management system. Here, we focus on both the performance indicators: the performance was evaluated in terms of temperature uniformity in the storage tank and the time taken to charge or discharge the system, (i.e. the phase change time), the cost was estimated, on the base of the experiments run on a small sample, on a 15 kWh LTES.

This paper focuses on a PCM-based thermal energy storage system comprised of a heat transfer fluid flowing in a tube wrapped in an annulus PCM-filled enclosure. This particular geometry was chosen because it has already been extensively investigated in the literature as it can be seen as the basic module for large shell-and-tube thermal storage. See, for example [15–19] and many more. As the benchmark case, pure PCM fully fills the annulus. For comparison purpose, three different enhancers, of the same weight, made of the same material (aluminium) were added to the PCM. Aluminum has been chosen for this project because the goal is to achieve a cost-effective solution. In particular, an aluminium wire mesh and aluminium chips (flakes) produced as waste products from machining operations were compared to the extensively studied and very expensive metal foams under the very same working conditions.

A prior study by the same authors published on the same Journal [20] examined various metal foams, highlighting one with superior characteristics. This study builds upon the previous findings, comparing cost-effective solutions to the previously selected superior foam.

A commercially available paraffin (Rubitherm RT40) was used as PCM in this study. Water is used as the HTF to charge or discharge the PCM annulus. A thorough parametric study was conducted where the water flow rate and temperature were systematically varied to study the influence of the working conditions on the charging and discharging times pertinent to the three aforementioned different enhancers.

Fig. 1. Experimental set up scheme.

1.1. Novelties introduced by the paper

- It presents new experimental tests that highlight the influence of flow rate and inlet HTF temperature. They can be used to calibrate numerical simulations, computational models, etc.;
- It proposes new cost-effective solutions that can help the development of LTES technology on the market. The use of chip had not been tested yet in the literature for applications such as this, and it was proved to be extremely effective;
- A sample of sufficient size was studied to serve as a model for real-world applications, in contrast to many works published in the literature that use only a few grams of the product;
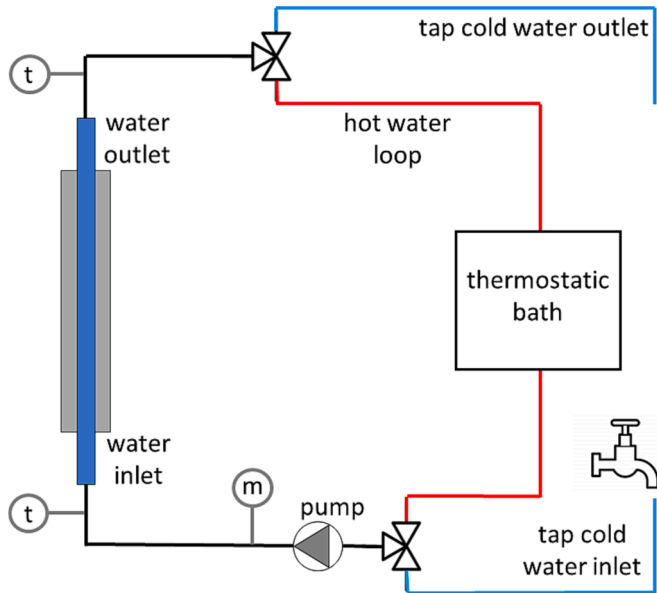- An economic analysis was conducted, emphasizing the advantages of choosing a compromise between cutting-edge and expensive

foams. Among them, Mustaffar et al. [8] proposed expanding aluminium metal mesh to accelerate the melting process of a PCM by approximately 14 %. The authors suggested that the improvement would be even greater if better thermal interfaces (such as soldering or brazing) were used to reduce the resistance to thermal contact. Similarly, Righetti et al. [9] tested the performance of a wire mesh-wrapped HTF tube charging a PCM-filled annulus. This costless solution eliminated the issue related to the void volume generation due to the paraffin volume change during melting and halved the melting time obtained without any enhanced surface. Ebadi et al. [10] tested a copper wire mesh added to a cylindrical LTES to observe that the addition of mesh leads to a uniform
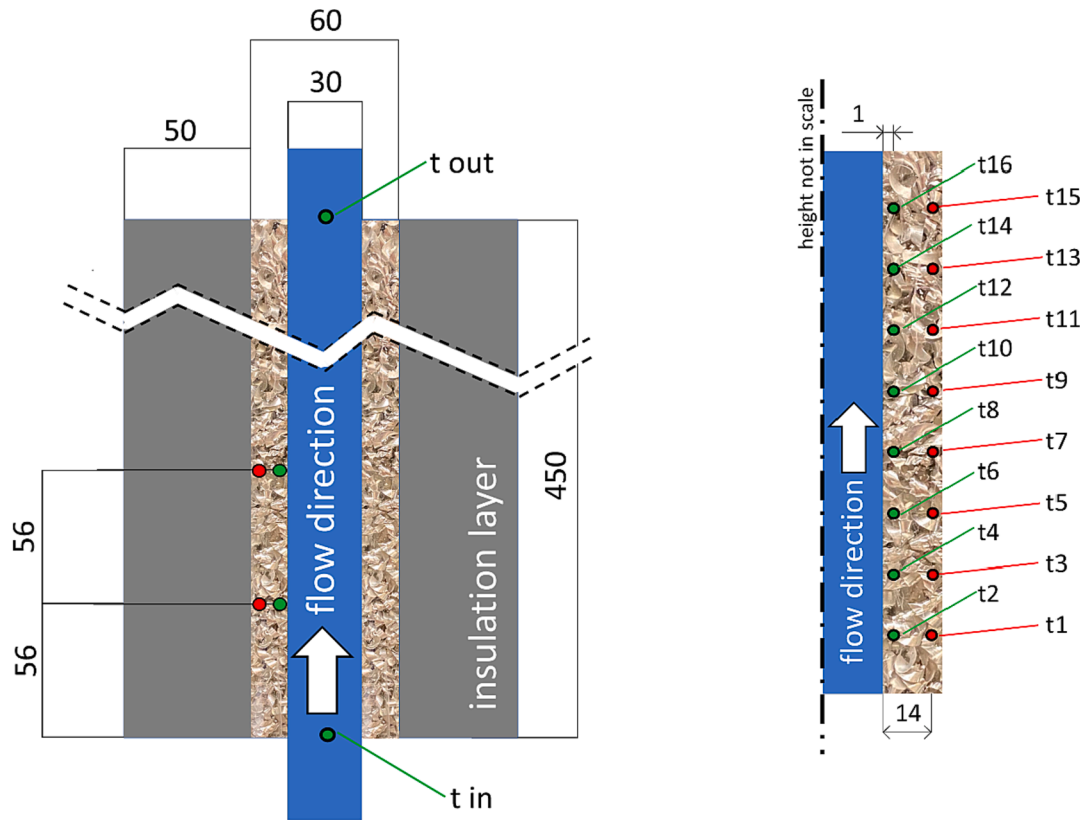
Fig. 2. A drawing of the tube-in-tube sample with the thermocouple positions, units in mm.

Table 1
Paraffin RUBITHERM® RT40 thermophysical properties as declared by the manufacturer.

Melting range: main peak 40 °C	38–43	°C
Congealing range: main peak 40 °C	38–43	°C
Heat storage capacity ± 7.5 % (temp. range: 38–43 °C)	165	kJ kg^{-1}
Specific heat capacity	2	kJ kg^{-1} K^{-1}
Solid density at 15 °C	880	kg m^{-3}
Liquid density at 80 °C	770	kg m^{-3}
Thermal conductivity (both phases)	0.2	W m^{-1} K^{-1}
Volume expansion	12.5	%

technologies, such as metal foams, and more economical standard solutions, such as latent storage without enhancers.

2. Experimental set up

A LTES (Latent Thermal Energy Storage), a PCM-wrapped HTF tube, was designed and built to analyse the thermal behaviour of a PCM during melting and solidification. Fig. 1 illustrates a schematic diagram of the experimental setup, which consists mainly of sample to be tested, hot and cold water loops, and data acquisition system. The hot water is produced by the thermostatic bath.

The sample is schematically shown in Fig. 2. It consists of two vertically arranged coaxial tubes (inner tube and outer tube) of 0.45 m in length; the main dimensions are shown in Fig. 2. The inner tube is made of aluminium. It has an inner diameter (ID) of 0.025 m and an outer diameter (OD) of 0.032 m, while the outer tube has dimensions of 0.056 m ID and 0.06 m OD and is made of plexiglass. The annulus between the tubes was sealed to create an enclosure to embed the PCM and the aluminium thermal enhancers. A 5-cm-thick insulating layer (thermal conductivity of flexible elastomeric foam (FEF) declared by the manufacturer 0.041 W m^{-1} K^{-1} at 0 °C) was wrapped around the plexiglass

tube to minimize heat loss to the surroundings. To measure the PCM local temperature distribution, 16 T-type thermocouples connected to a K170 ice point reference (with stability of ± 0.005 °C and precision of ± 0.005 °C) were inserted into the PCM cavity. Their position is also shown in Fig. 2. All thermocouples were calibrated against a reference thermoresistance, so a maximum uncertainty equal to ± 0.1 K is anticipated. The outer Plexiglass tube was drilled to allow the thermocouple wires to enter in the PCM enclosure, and then the holes were glued with epoxy resin to prevent liquid PCM leakage. To monitor the temperature field at different heights and depths, half of the thermocouples are set closer to the inner pipe (marked by green circles in Fig. 2) while the other half (red circles in Fig. 2) are at the outer wall. Each pair of thermocouples (red and green on Fig. 2) are 5.6 cm apart from the adjacent one. Besides, two extra thermocouples were fixed on the outside of the outer pipe to investigate the wall temperature and estimate the heat loss to the surroundings.

The hot HTF circuit was designed to feed the sample with water at a constant temperature during the charging cycle. An electric heater connected to a controller allowed the water temperature to be regulated with a stability of ± 0.2 °C. In contrast, the cold HTF loop delivers tap water to the sample (blue line in Fig. 1). Water flow rate was measured using an electromagnetic flowmeter "Promag 50 W" by Endress + Hauser while water temperature was measured by a T-type thermocouple. Finally, a thermopile was placed between the inlet and outlet of the test module to measure the water temperature rise or drop during discharge and charge, respectively. In all our testes, water flowed upward in the inner tube to ensure that even at the lowest flow rates, it could still fill the entire section, avoiding annular flow.

All measured values are recorded at 1 Hz using an Agilent 34970A data acquisition system and processed by LabVIEW software.

RUBITHERM® RT40, a commercially available paraffin wax, was selected as PCM to be used in all tests. As reported by the manufacturer, this PCM is characterised by an almost isothermal solid–liquid phase-
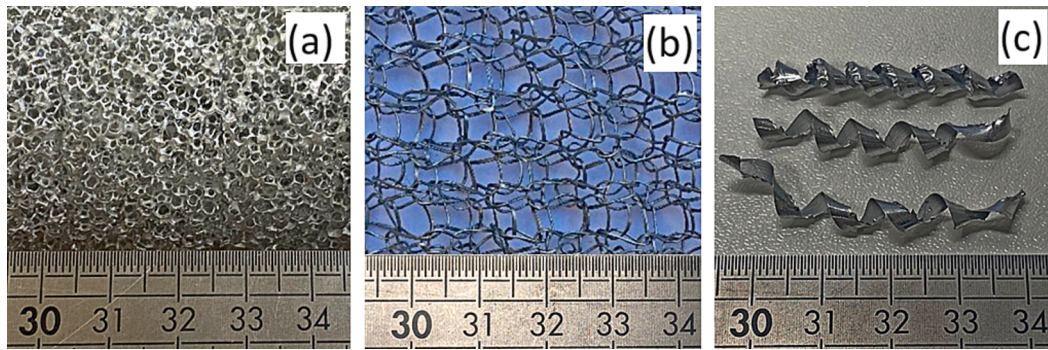
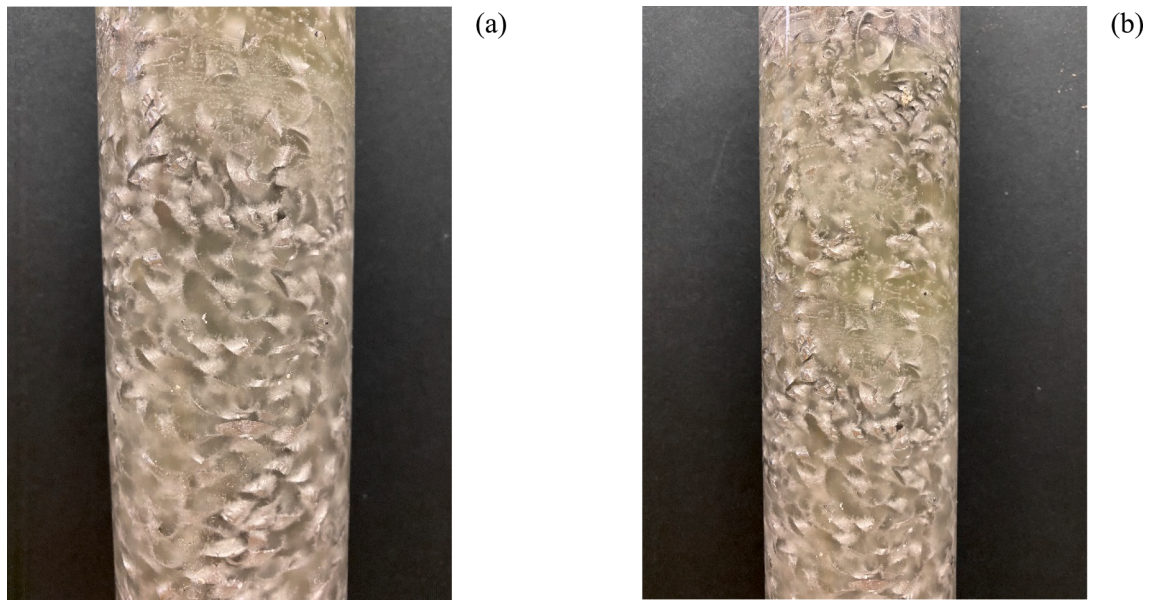**Fig. 3.** A picture of the 10 PPI foam (a), wire mesh (b) and chip (c).

Fig. 4. A picture of the chip sample before (a) and after (b) 10 complete cycles.

Table 2
Uncertainty of the measurement devices.

Device/Measure	Uncertainty	Notes
T-type thermocouple	±0.1 K	Calibrated in the lab
T-type thermopile	±0.05 K	Calibrated in the lab
K170 ice point reference	Stability ± 0.005 K Precision ± 0.005 K	Calibrated by the manufacturer
Promag 50 W flowmeter	±0.5 % of the reading	Calibrated by the manufacturer
Thermostatic bath	Temperature stability ± 0.2 K	Calibrated in the lab
Climatic room	Temperature stability ± 0.2 K	Calibrated by the manufacturer
Agilent 34,970 A data acquisition system	Accuracy ± 0.004 % of the reading Frequency accuracy ± 10 ms	Calibrated by the manufacturer
Energy on the water side (Eq.2)	Max. 5 % of the value	Kline and McClintock
Energy loss (Eq.1)	Max 12 % of the value	Kline and McClintock

change process with excellent stability after many charge–discharge cycles. It is chemically inert, nontoxic, recyclable and low cost (approximately 2.5 € kg^{-1}). The most relevant thermal and physical characteristics provided by the manufacturer are summarised in Table 1.

In all of our experiments, 600 g of the same PCM was tested and embedded in the annulus. The first set of experiments, conducted as a benchmark test, were pure PCM tests.

All thermal enhancers were made of aluminium (density = 2700 kg m^{-3}; thermal conductivity = 220 W m^{-1} K^{-1}) with an equivalent solidity of 5 % (aluminium volume/available volume).

In a previous study, three different metal foams were tested [20]. Among those, the sample containing 10 PPI foam and 731 m^2 m^{-3} of surface area per unit volume was selected to represent one of the most efficient solutions and therefore to compare the results of the proposed cost-effective solutions presented in this document. Here, two other samples were prepared, tested, and evaluated. In the first, an insert generated by wrapping a sheet of commercial aluminium wire mesh (600 mm x 700 mm) commonly used for air filters was embedded in the PCM annulus. The average thickness of the wire is 0.9 mm with average cell dimensions being around 7 mm x 6 mm. Finally, as an alternative option, a total of 7075 aluminium chips (flakes) were used as enhancers in the PCM-filled annulus: the average chip length is 40 mm, the average width 3 mm, and the average thickness 0.4 mm.

In the latter two cases presented here, unlike the previously tested foams, the porous structure was not brazed to the inside tube wall to minimize the cost while allowing for a simple and easy-to-implement enhancers. To put things into prospective, the current price of wire mesh is about 4 € kg^{-1} while that of chips is 0.5 € kg^{-1}. The total cost (in euros) for the material needed for different enhancers studies here was about 0.05 € for the chip, 0.40 € for the mesh, and 20 € for the foam (enhancers are shown in Fig. 3). This gain in price and simplicity in

Table 3
Repeatability tests.

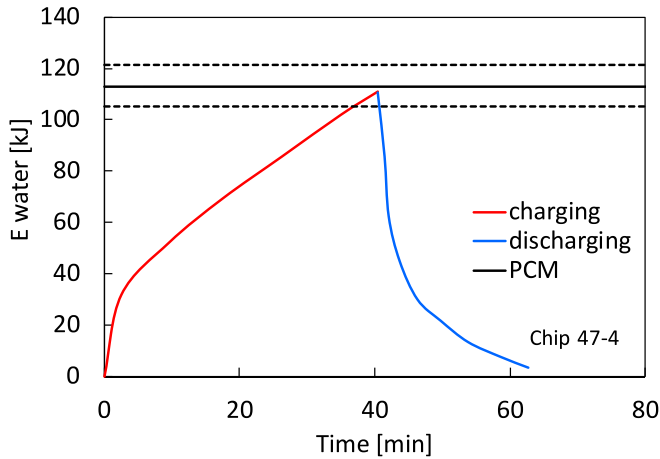|	Total charging time (47–4 test) [min]	Total discharging time (16–4 test) [min]	Average PCM temperature at the end of the charging process [°C]
PCM + foam	11.9–12.0–11.8–11.9	8.0–7.9–7.8–8.1	41.6–42.0–41.9–41.5
PCM + chip	38.7–39.2–39.0–38.5	22.8–22.5–23.1–23.3	42.3–41.9–42.5–42.7
PCM + wire mesh	93.0–92.6–94.2–93.7	28.3–28.0–28.6–28-4	43.1–42.6–43.3–42.9
PCM only	126.1–127.3–126.9–124.5	42.8–42.3–43.4–43.0	44.6–45.1–45.3–44.2

Fig. 5. Energy stored during the charging time and released during the discharging for the PCM + chip sample.

Table 4
Time in minutes taken for the charging and discharging processes of different tests.

Test name	HTF flow rate [l min^{-1}]	HTF inlet temperature [°C]	PCM + foam PC length [min]	PCM + chip PC length [min]	PCM + wire mesh PC length [min]	PCM only PC length [min]
		charging process				
55-4	4	55	6.2	26.0	37.4	70.2
51-4	4	51	7.9	31.6	49.7	93.0
47-4	4	47	11.9	38.7	93.0	126.1
45-4	4	45	16.0	71.6	135.4	160.4
		charging process				
47-2	2	47	17.5	54.6	101.4	127.9
47-4	4	47	11.9	38.7	93.0	127.6
47-6	6	47	9.7	38.3	67.1	122.6
47-8	8	47	8.7	37.5	62.7	121.4
		discharging process				
16-2	2	16	12.4	25.6	33.6	46.7
16-4	4	16	8.0	22.8	28.3	42.8
16-6	6	16	7.1	22.3	21.7	43.2
16-8	8	16	6.3	21.7	19.0	45.3

distributed in the annulus. The gap was measured only in few points in the frontal section of the setup, since it was the only reachable with a calliper. The average value was around 0.2 mm in the chip case and around 0.3 mm in the metal mesh case. According to [21], the effect of this thermal resistance should detriment the melting and solidification time between 50 % and 60 %.

As a final remark, to achieve the required porosity, the amount of chips/metal wire inserted in the annulus is very high and they are strongly intertwined with each other. As a result, the material is neither displaced nor compressed during one or more cycles even because only gravity occurs on the system. Fig. 4 shows the material before and after the completion of 10 complete cycles to demonstrate that there is hardly any visual difference between the two. Pictures were taken at ambient temperature when the PCM was totally solidified.

3. Experimental test procedure

Each test can be subdivided into two phases: the charging phase (includes melting) and the discharge phase (includes solidification). Initially, 20 °C HTF flows inside the LTES to ensure a uniform starting temperature throughout the system. Then, the charging phase begins. Hot water is circulated inside the inner tube until the PCM is completely melted. The criterion for considering this phase concluded is when all thermocouples inserted in the PCM measure a temperature greater than 41 °C. Because the outer tube is made of Plexiglas, during a preliminary test run without the insulation layer, it was possible to physically observe and check that no solid PCM zones were present at the end of the charging phase. The discharge phase begins when all the thermocouples measure a temperature higher than 41 °C. Note that to obtain an almost homogeneous temperature starting condition, water at around 42 °C was circulated before the beginning of the discharging phase. So, the average PCM temperature at the beginning of this phase, when the cold HTF starts to flow into the inner tube, was around 41 °C (deviations within 0.7 °C were measured). This process is concluded when the PCM, after solidification, reaches an average temperature of 20 °C.

In this paper, several tests were conducted as subdivided into two main groups. In the first group, the flow rate was kept constant at 4 l min^{-1} to study the effect of the inlet HTF temperature which was varied over 45, 47, 51, and 55 °C. In the second group, the inlet HTF temperature was fixed at 47 °C to study the effect of the flow rate varying from 2 to 8 l min^{-1}. (at l min^{-1} interval). With the discharge tests, nonetheless, the inlet HTF temperature was fixed at 16 °C to simulate tap water where four flow rates were tested: 2, 4, 6, and 8 l min^{-1}. Table 2, among many other data, summarises the working conditions of all the tests performed.

3.1. Uncertainty, repeatability and error analysis

Table 2 lists the uncertainties declared for all the measurement devices used during the experiment and the maximum value of the total uncertainty of power and energy evaluated according to the Kline and McClintock [22] method.

Furthermore, to ensure the quality of the measurement, a few repeatability tests were run. In particular, the 47–4 test was repeated 4 times for each sample. Table 3 summarizes the total charging and discharging times and the average PCM temperature at the end of the

design come at the expense of additional thermal contact resistance which lowers the heat transfer, as documented in the literature; see for example [8] or Opolot et al. [21] who proposed a theoretical model, backed by numerical simulations, to quantitatively evaluate the effect of thermal contact resistance of such systems. The authors summarised that the contact resistance is strongly dependent on the width of the gap between the heated tube and the metallic structure. The time loss in charge/discharge performance when compared to a tightly attached metal insert case could range from around 3 times considering a 1 mm contact resistance gap to more than 15 times if a 10 mm gap is taken into account. In this experiment the gap width was difficult to accurately measure, since the metallic mesh and the chips were randomly
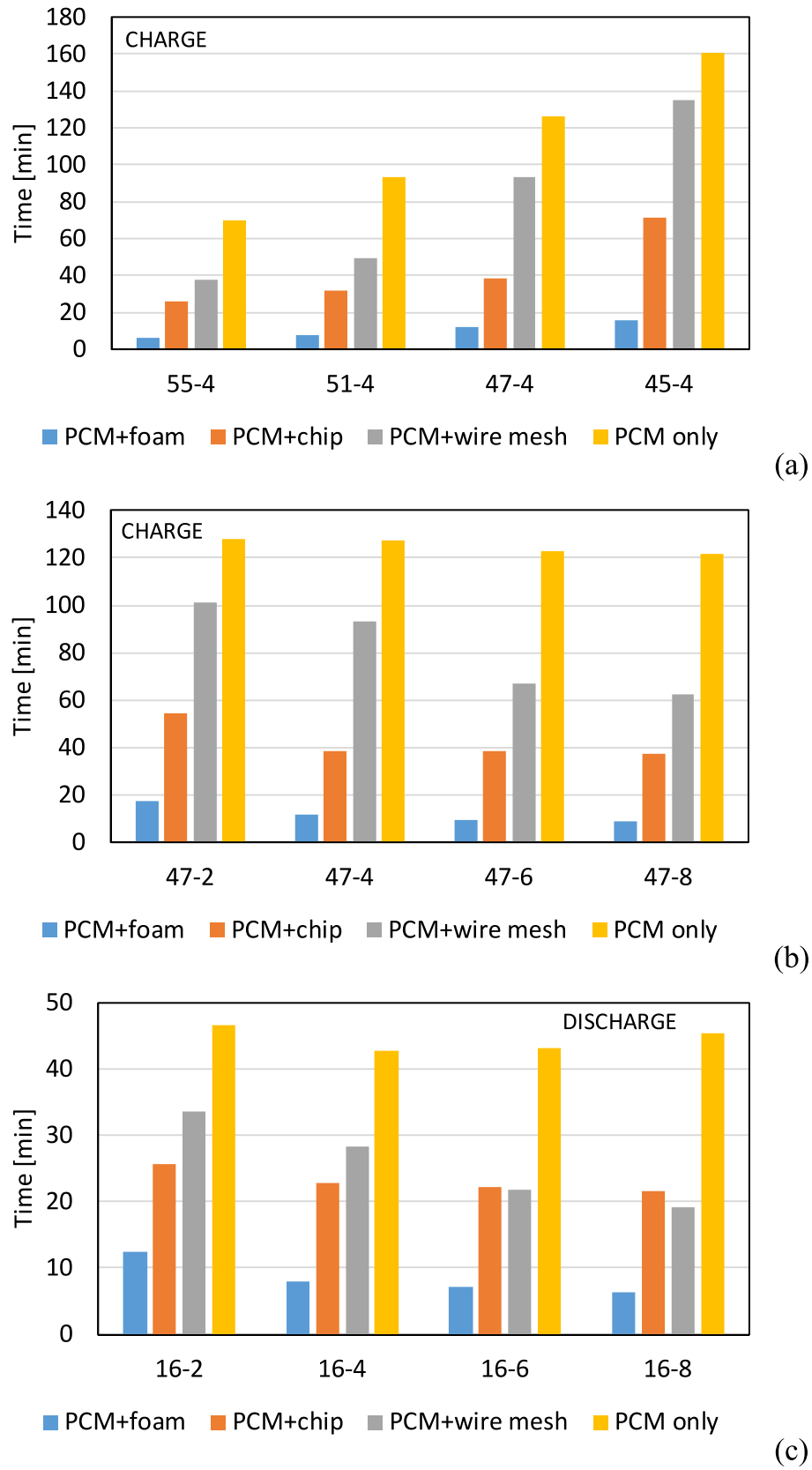
Fig. 6. Operation times of different tests in the four samples. (a) charging at 4 l min^{-1} flow rate; (b) charging at 47 °C HTF temperature; and (c) discharging at 16 °C HTF temperature.
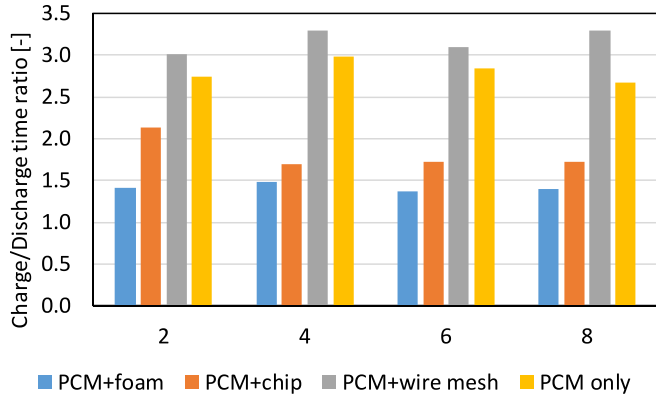
Fig. 7. Charge / discharge time ratio in the four samples at different flow rates. The temperature of the inlet HTF during charging = 47 °C, the temperature of the input HTF during discharging = 16 °C.

charging process. On average, errors below 2 % were detected comparing the charging and discharging times, and below 3 % considering the average PCM temperatures.

Finally, the heat losses to the surroundings were evaluated by means of the measure of the temperature of the outside insulation layer of the outer pipe according to Eq. (1) where the ambient temperature was kept constant at 20 ± 0.2 °C and a natural convection heat transfer coefficient α of 5 W m^{-2} K^{-1} was considered. The amount of energy lost during each test was compared to the energy released by water (Eq. (2)) defining a percentage error (Eq. (3))

$$E_{loss} = \sum_{\tau_0}^{\tau_{end}} \alpha A \left(t_{wall} - t_{air}\right) \tag{1}$$

$$E_w = \sum_{\tau_0}^{\tau_{end}} \dot{m}_w \, c_{p,w} \left(t_{w,in} - t_{w,out}\right) \tag{2}$$

$$\varepsilon = \left(\frac{E_w - E_{loss}}{E_w}\right) \tag{3}$$

The maximum percentage error was observed in the reference sample tests since they were the longer runs. The maximum value was 3.7 %, while the average value of all the test campaign 2.4 %.

To further validate the test rig, Fig. 5 presents the energy stored during the charging time and released during the discharging for the PCM + chip sample. Due to space constraints, only the results of this sample are presented here. The stored energy for this specific test, assessed according to Equation (2), was 110 kJ. The related uncertainty is rather high since the average water temperature difference is 0.4 ± 0.1 K.

Theoretically, the 0.6 kg of the chosen PCM should account for 92 kJ $\pm$ 7.5 % of latent energy when transitioning from 38 °C to 43 °C (refer to Table 1, which includes data provided by the manufacturer). Additionally, sensible heat was stored by the PCM when raising its temperature from 20 °C to 43 °C, estimated to be around 22 kJ; however, there were insufficient data available to assess the uncertainty of this value. Therefore, a total energy of approximately 114 $\pm$ 7.5 % kJ should be stored by the PCM. During the discharging phase, the water absorbed approximately 107 kJ of energy (Equation (2). The discrepancy of about 3 kJ from charging to discharging can be attributed to energy losses to the environment. Furthermore, the mismatch between the water side and PCM side was a result of measurement uncertainty and uncertainties in the thermophysical properties of the PCM.

4. Experimental results

Table 4 contains the times (measured in minutes) taken to charge and discharge for all tests conducted here. The same data have been represented in diagrams (Figs. 6 and 7) for a more comprehensive

understanding of the problem. X axis of the plots reports the test name as mentioned in Table 2. One immediately notes that, as expected, the pure PCM sample (i.e. those with no enhancer) took the longest to charge and discharge, on average + 160 % longer than the PCM + chip and + 50 % longer than the PCM + wire mesh and 900 % longer than the PCM + foam. This, once again, signifies the addition of high-conductivity material to PCM as they shorten the operating time (despite significant contact resistance between some enhancers and the heated/cooled surface). Moreover, the PCM + foam sample speeds up charging and discharging the most (the process is on average about 3.5 times shorter than PCM + chip and about 6 times shorter than PCM + wire mesh). This result is again expected, but this amazing heat transfer coincides with such high material cost (orders of magnitude comparatively) that hinders their deployment in large scale industrial applications. Furthermore, foam was brazed, an expensive process that promotes an even better heat transfer performance as discussed in Olopot et al. [21]. A detailed analysis of the PCM + foam sample tests can be found in our previously published paper [20].

In search for an alternative, we shift our attention to aluminium chips and wires. Interestingly, chips show superior results compared with those of the wire mesh. In fact, the wire mesh shortens the charging time by about 50 % and the discharging time by 70 % compared to those of pure PCM. With chips, the charge and discharge time are shortened by 180 % and 90 %, respectively, compared with those of pure PCM. These results are even more interesting since both chips and wires were not brazed to the tube. According to [21] a further improvement in the melting and solidification time between 50 % and 60 % should be reached if they had been brazed on the heat transfer tube.

Throughout the process, the aluminium inserts heat (or cool) faster than the PCM due to their higher thermal conductivity. Consequently, the PCM is heated (or cooled) by both the HTF tube and the metal structure. In the absence of enhancers, the pure PCM would extend the process, also due to material shrinkage; for further details, refer to Zhao and Hooman in Mobedi et al. [1].

The most advantageous condition for working with wire mesh is 47–8 (i.e., charging at high flow rates), while the condition where the advantages are most limited are 47–2 and 45–4 (i.e. charging at low flow rates or at low temperature differences). Analogous results were obtained with the chip sample.

As Table 4 indicates, the case 45–4 is slowest among the cases with fixed hot water flow rate and variable hot water inlet temperature. However, case 47–2 is the slowest among the cases with fixed inlet temperature and variable flow rate. With discharge, however, all cases struggle with the lowest flow rate. The shortest discharge time is obtained at the highest flow rate except for the pure PCM where the discharge time shows a non-uniform response to the flow rate. Like all other cases, the pure PCM experiences the longest discharge at the lowest flow rate but then with doubling the flowrate, the time plunges to minimum and further increase in flowrate, appears to be unhelpful. Probably because the main resistance to heat transfer is on the PCM side, so the system does not respond to an increase in flowrate.

In general, chip can reduce charging and discharging times more than wire mesh, most likely because their geometry provides a broader section for heat transfer, thereby enhancing the efficiency of thermal exchange, as acknowledged by the theory of heat transfer through fins and extended surfaces. Only at higher flow-rate discharge conditions the total phase change times for these two enhancers are almost equivalent. The chip heat transfer cross section is larger than that of the wire mesh, in fact, the wire mesh has an average wire diameter of 0.9 mm, while with the chip the average width is 3 mm. All in all, the chips conduct heat more efficiently, and this becomes a more efficient phase-change process.

At the same flow rate, the discharge times are always shorter than the charge times, this is because the temperature difference between HTF and PCM is higher in the discharge where water at 16 °C is used.

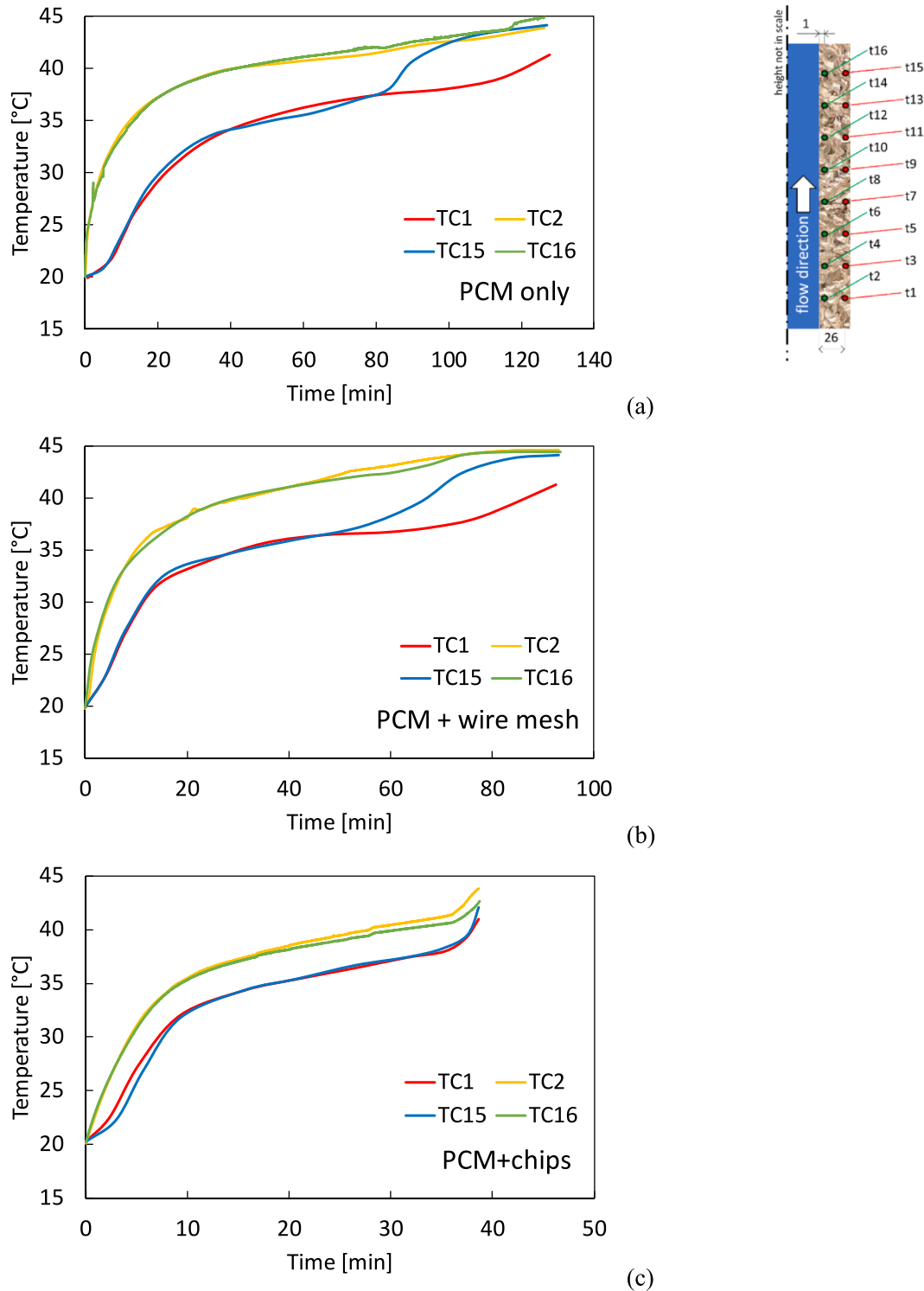However, not all solutions affect charging and discharging times in

Fig. 8. Local temperature in the PCM during the charging phase of the 47–4 test (a) PCM only (b) PCM + wire mesh (c) PCM + chip (d) PCM + foam.

the same way. To further investigate this, the comparison between the charging and discharging time for each sample as a function of flow rate is presented in Fig. 7.

When using only PCM, the charging time is about 2.8 times the discharging time. The process is mainly controlled by conduction, and the higher the temperature difference, the faster the process. When using foam, the numerical value of the ratio of charging time to discharging time is on average 1.4. This means that foam reduces the charging time

(which includes the melting process) much more than the discharging time. In fact, the heat transferred by the metal ligaments is able to penetrate the inner part of the solid material more effectively, enhancing conduction while limiting the convection, and exchanging heat more homogeneously throughout the volume. During solidification, this capability is limited because, as already demonstrated by [23,24], in small cavities, as in the present case, the metal foam mostly affects the conduction, limiting the convection.
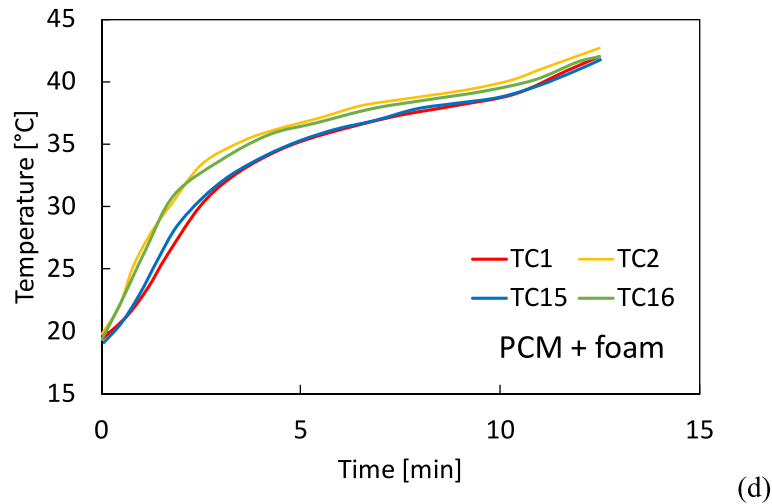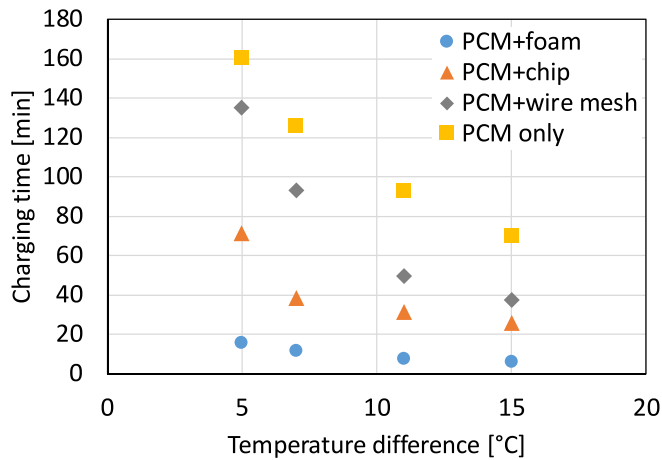
Fig. 8. (*continued*).

Fig. 9. Charging time for the four samples as a function of the temperature difference between inlet HTF temperature and PCM phase change temperature. Flow rate 4 l min^{-1}.

A similar effect should occur also in chips. In fact, when used, chip reduces the charging time more than the discharging time (the average charge/discharge ratio is about 1.7). As described before, the thick aluminium pieces dispersed in the PCM generate a complex 3D structure of closely intertwined and tangled fibres that touch each other in several areas even if not brazed, being able to transfer heat efficiently by conduction. This is confirmed by the fact that the performance is closer to that of the foams rather than to that of the wire mesh. Finally, wire mesh reduces charging time and discharging time proportionally, which means that the efficiency of the wire mesh is quite low and the process improvement is proportional to the heat transfer area enhancement, resulting in a charge/discharge ratio similar to that of PCM only.

4.1. Local temperature analysis

It is well known that the addition of metal items to a PCM storage is able to make the temperature field more homogeneous [7]. In addition, in this case, both the use of chip and wire mesh succeed in reducing the temperature gradients within the sample. For the sake of clarity, Fig. 8 shows only the temperatures recorded at the bottom, close to the HTF inlet (TC1 and TC2), and at the top, close to the HTF outlet (TC15 and TC16) of the section during the 47–4 test for the four samples. As shown in Fig. 2, the odd-numbered thermocouples are placed near the external

PCM layer and the even ones close to the inner tube where the HTF flows. Thus, not all the thermocouples are shown in these graphs, but since the phase change process proceeds radially and from the bottom to the top, their values fall within those plotted here.

In the PCM only case, a negligible temperature difference between bottom and top (less than 1 K) regions is measured until almost the completion of the test: this is mainly due to the fact that the water temperature variation is rather limited (approximately 0.25 K). Therefore, this operating condition implies an almost uniform temperature profile along the tube. However, after 80 min, a sudden increase in the temperature measured by TC15 can be observed. This can be explained by considering that during the phase change, the hot liquid moves upward as a result of the density variation, and thus the phase change process proceeds from the top. One can assume that the rising liquid reaches the top wall and turns as pulled by gravity. This heated liquid flow reaches the location of T15 and increases the local temperature close enough to that of T16 after almost 20 min. Apparently, this is not long enough for the same heated stream to reach the location of TC1 where a solid layer is formed (shrinkage). A similar behaviour is noted for wire mesh (but starting at about 60 min instead of 80 as was the case for pure PCM).This means that after around 80 min, the solid/liquid front moving downwards reaches TC15. A similar behaviour was also observed during the tests with wire mesh. In contrast, chips and foam conduct heat through the sample more evenly. As a result, no sudden changes in temperature can be detected.

Moreover, a radial temperature gradient caused by the low thermal conductivity of the PCM can be observed. In the PCM-only case, the average difference between the internal and external temperature is 7 K; this is reduced to 5 K in the case of PCM + wire mesh case 5 K, to 3 K in the case of PCM + chips, and to less than 1 K in the PCM + foam sample.

4.2. Analysis of operating conditions

During the charging phase, four HTF input temperatures were considered: 55 °C, 51 °C, 47 °C, and 45 °C to study the effect of the inlet HTF temperature. Temperature differences between the phase change temperature of the PCM and the inlet HTF temperature of 15 K, 11 K, 7 K, and 5 K were analysed. Fig. 9 shows the charging time as a function of this temperature difference for each sample. As expected, as the water temperature increases, the charging time decreases. The PCM-only is the sample that is least influenced by variations in HTF temperature. It increases the charging time by 2.3 times when varying from a temperature difference of 15 K to 5 K. On the other hand, the most affected case is the wire mesh sample with a variation of 3.6 times under the same working conditions. Differently, foam and chip samples showed similar
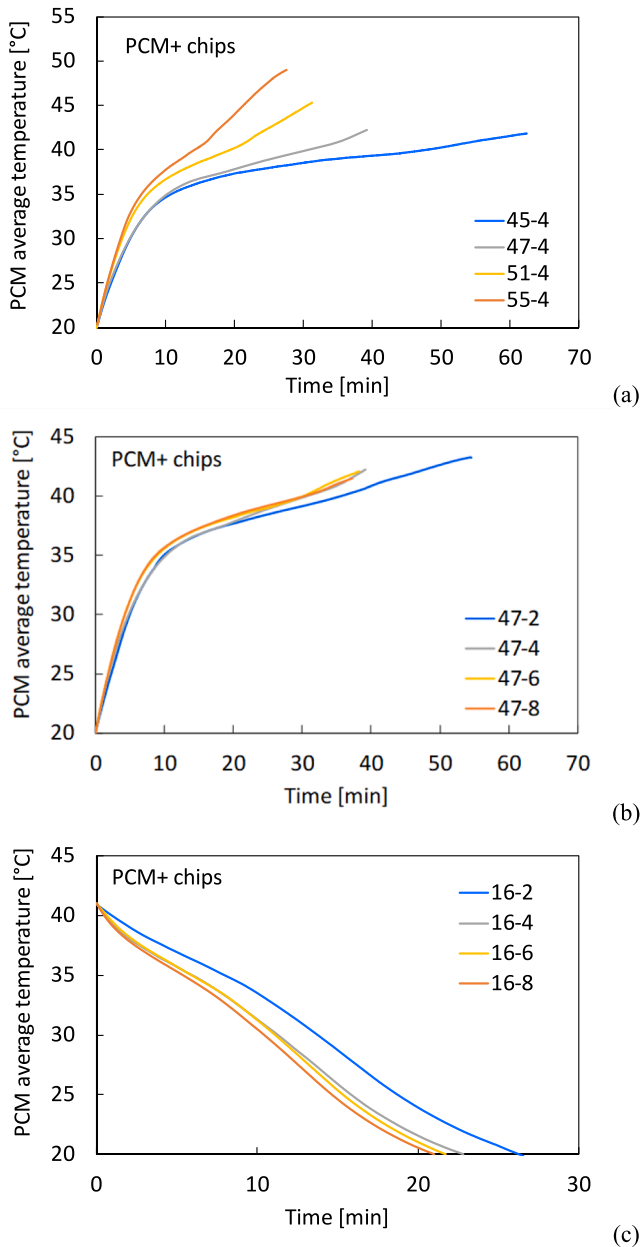
Fig. 10. PCM average temperature in the PCM + chip sample during (a) charging at constant flow rate of 4 l min^{-1} (b) charging at constant inlet HTF temperature of 47 °C (c) discharging at constant inlet HTF temperature of 16 °C.

less than 20 % when the temperature difference is 5 K, while it shortens the time around 90 % when it comes to 15 K temperature difference. Consequently, it becomes even more important to define the correct working conditions for a given PCM.

The charging and discharging times of tests carried out at the same temperature and different flow rates are then analysed. The case of the PCM + chip sample is shown in Fig. 10, which shows the average temperature during the charging and discharging phases, respectively. These tests on chip show comparable charging and discharging times when flow rates between 4 and 8 l min^{-1} are used (difference in time between the three conditions around 2 min over 1 h cycle) furthermore the average PCM temperature profiles measured are almost the same. While when the flow rate is 2 l min^{-1} the total cycle time is around 33 % longer compared to the other investigated flow rates and the average temperature of the PCM remains about 4 K higher during the discharging process. This can be explained considering that at the lowest HTF flow rate, the flow tends to be laminar (Re 1700), whereas at higher flow rates, it develops towards transitional / turbulent flow. Therefore, the heat transfer performance on the water side varies with Reynolds number and affects the phase-change process.

Similar behaviour was also observed in the tests carried out on the other samples in which a metal wire mesh (and even foam) was added, as can be deduced from the charging and discharging time data reported in Table 2. On the other hand, the tests carried out on the PCM only sample were not affected by the variation in the HTF flow rate, even when this was reduced to 2 l min^{-1}. In fact, all four tests at different flow rates show very similar charging and discharging times (within approx. 5 %). Therefore, in this case, it can be stated that the dominant heat transfer resistance is on the PCM side, so the effects of the thermal resistance on the variation of the water side are negligible.

Finally, as it can be seen in Fig. 10c, the profiles do not show any plateau during the solidification. This can be explained considering that during the solidification process, temperature difference between the inlet water and PCM is quite high (24 K) which, combined to the extended surface used and to the limited amount of PCM, make the heat transfer so fast that the plateau disappears. Similar results had already been found by the present authors in several works, among them it is worth citing Righetti et al. [9].

4.3. Cost analysis

As a case study example, the calculation of an LTES of approximately 15 kWh is proposed. This size can be used as storage for a residential building that is coupled to a heat pump for heating purposes. The main results are listed in Table 5.

The cost of the LTES based on the PCM only technology, consisting of 300 kg of PCM (RT40 by Rubitherm) contained in 500 tubes equivalent to the tested sample, is approximately €1950. The commercial price of the material is 5 € kg^{-1} and the tubing structure costs about 450 €. The addition of metal material (5 % of the volume, that is 50 kg of aluminum) reduces the amount of PCM used in storage, and thus also the heat storage capacity of the LTES that goes from 15.05 kWh to 14.30 kWh. It also increases the cost, which is estimated at around 2075 € (PCM + wire mesh case), around 1900 € (PCM + chip case), and around 11,875 € (PCM + foam case). So, it was possible to estimate the investment cost

enhancement around 2.8 times. In other words, these results demonstrate that the wire mesh is a solution capable of shortening the charging time only when subjected to high HTF-PCM temperature differences. In fact, as compared to the PCM-only sample, it reduces the charging time

Table 5
Cost analysis of a 15 kWh case study.

	PCM cost €	Metal insert cost €	Total cost €	total energy stored kWh	cost per stored energy € kWh^{-1}	average time estimated for 1 cycle min	cost per energy stored in a cycle € kWh^{-1}
PCM only	1500	–	1950	15.05	130	190	205
PCM + foam	1425	10,000	11,875	14.30	831	20	138
PCM + chip	1425	25	1900	14.30	133	75	83
PCM + wire mesh	1425	200	2075	14.30	145	140	169

per amount of stored energy, expressed as € kWh^{-1}. Being the foam the most expensive material, it derives in the most expensive storage under this point of view.

Obviously, by means of the insert addition, the charging and discharging times of the storage decrease considerably. In this case a round trip cycle (charging + discharging) was taken into account for the analysis. The cycle time was not measured experimentally, but it was evaluated on average working conditions on the base of the experiment run with the single tube samples. According to the results presented in this paper, the foam takes the shortest time, followed by the chip and the wire mesh. The PCM only set up took the longest time to complete a total charging + discharging cycle.

Finally, the cost per energy stored in a cycle was evaluated as the ratio between the total cost multiplied by the average time estimated for one cycle and the total energy stored. This number summarises the investment cost, the storage capacity and the velocity in storing and releasing energy. The smallest, the better. So under this point of view, the chip solution outperformed the other options.

Obviously, these are only preliminary results, but it is already possible to conclude that the addition of chips seems to be the most cost-effective solution to increase the average thermal conductivity of the system while keeping costs down. Further analyses are required to size a system that can be offered on the market.

5. Conclusions

It is generally recognised for many technical applications that increasing the average thermal conductivity of PCM can provide benefits including reduced charging and discharging times and a more homogeneous temperature field within the PCM. A prior study by the same authors published on the same Journal [20] examined various metal foams, highlighting one with superior characteristics. This article proposes two possible cost-effective and feasible solutions to increase thermal conductivity: the use aluminium chips and of aluminium wire meshes.

The proposed solutions were applied to an LTES consisting of 600 g of commercial PCM (RT40) that changes temperature at about 40 °C inserted into the annulus of a tube-in-tube heat exchanger. Water flows inside the inner tube.

Four samples were studied: the first, used as a reference, involves the use of PCM only in the annulus. The other three, in addition to the same amount of PCM, contain 5 % of the volume of aluminium in different forms: foam, chip, or wire mesh (density 95 %). The times of the charging and discharging processes and the temperature range within the PCM were measured and compared as the temperature and flow rate of the inlet water was varied. The flow rate was set to vary between 2 and 8 l min^{-1} and the temperature between 45 and 55 °C.

The main results can be summarised as follows:

(1) The PCM-only sample exhibited the longest charging and discharging times, while the PCM + foam sample shortened them the most. The two cost-effective solutions (chip and wire mesh) resulted in intermediate phase change times. To further improve the performance of chip and wire mesh, metal structures could be brazed on the HTF tube. In this way the gap thermal resistance should be eliminated and the melting and solidification time further reduced between 50 % and 60 % [21]

(2) On average, the chip was able to reduce charging and discharging times more than wire mesh probably due to its greater heat transfer cross section.

(3) The four solutions presented a similar behaviour in terms of PCM temperature gradient reduction. In the PCM-only case, the average difference between internal and external temperature was 7 K, in the PCM + wire mesh case 5 K, and in the PCM + chips case 3 K.

(4) All samples reduce the phase change time if the HTF flow rate and the temperature difference between HTF and PCM increased. At low flow rates (2 l min^{-1}), the HTF flow regime tended to be laminar, so the variation of charging and discharging times was more than linear. This was due to the thermal resistance on the effects of the water side.

(5) The cost analysis of a 15 kWh system based on the tested sample demonstrates that these two cost-effective thermal conductivity enhancing solutions can become a key enabling method to widely deploy latent thermal energy technology widely in many different applications. In fact, they present the best trade-off between costs and performance expressed in terms of "cost per energy stored in a cycle"

CRediT authorship contribution statement

Giulia Righetti: Conceptualization, Data curation, Formal analysis, Funding acquisition, Investigation, Methodology, Project administration, Writing – original draft, Writing – review & editing. **Claudio Zilio:** Conceptualization, Data curation, Formal analysis, Funding acquisition, Investigation, Methodology, Project administration, Writing – original draft, Writing – review & editing. **Kamel Hooman:** Conceptualization, Data curation, Formal analysis, Funding acquisition, Investigation, Methodology, Project administration, Writing – original draft, Writing – review & editing. **Simone Mancin:** Conceptualization, Data curation, Formal analysis, Funding acquisition, Investigation, Methodology, Project administration, Writing – original draft, Writing – review & editing.

Declaration of competing interest

The authors declare that they have no known competing financial interests or personal relationships that could have appeared to influence the work reported in this paper.

Data availability

No data was used for the research described in the article.

Acknowledgments

References

[1] M. Mobedi, K. Hooman, W.-Q. Tao, Solid-Liquid Thermal Energy Storage Modeling and Applications, 1st ed., CRC Press Taylor and Francis Group, 2022.

[2] S. Wu, T. Yan, Z. Kuai, W. Pan, Thermal conductivity enhancement on phase change materials for thermal energy storage: A review, Energy Storage Mater. 25 (2020) 251–295, https://doi.org/10.1016/j.ensm.2019.10.010.

[3] C. Zhao, M. Opolot, M. Liu, J. Wang, F. Bruno, S. Mancin, K. Hooman, Review of analytical studies of melting rate enhancement with fin and/or foam inserts, Appl. Therm. Eng. 207 (2022), https://doi.org/10.1016/j.applthermaleng.2022.118154.

[4] C. Xu, H. Zhang, G. Fang, Review on thermal conductivity improvement of phase change materials with enhanced additives for thermal energy storage, J. Energy Storage. 51 (2022), https://doi.org/10.1016/j.est.2022.104568.

[5] Z. Khan, Z. Khan, A. Ghafoor, A review of performance enhancement of PCM based latent heat storage system within the context of materials, thermal stability and compatibility, Energy Convers Manag. 115 (2016) 132–158, https://doi.org/10.1016/j.enconman.2016.02.045.

[6] M.M. Heyhat, S. Mousavi, M. Siavashi, Battery thermal management with thermal energy storage composites of PCM, metal foam, fin and nanoparticle, J. Energy Storage. 28 (2020), https://doi.org/10.1016/j.est.2020.101235.

[7] J. Shi, H. Du, Z. Chen, S. Lei, Review of phase change heat transfer enhancement by metal foam, Appl. Therm. Eng. 219 (2023), https://doi.org/10.1016/j.applthermaleng.2022.119427.

[8] A. Mustaffar, A. Harvey, D. Reay, Melting of phase change material assisted by expanded metal mesh, Appl. Therm. Eng. 90 (2015) 1052–1060, https://doi.org/10.1016/j.applthermaleng.2015.04.057.

[9] G. Righetti, R. Lazzarin, M. Noro, S. Mancin, Phase change materials embedded in porous matrices for hybrid thermal energy storages: Experimental results and modeling, Int. J. Refrig 106 (2019) 266–277, https://doi.org/10.1016/j.ijrefrig.2019.06.018.

[10] S. Ebadi, S.H. Tasnim, A.A. Aliabadi, S. Mahmud, An experimental investigation of the charging process of thermal energy storage system filled with PCM and metal wire mesh, Appl. Therm. Eng. 174 (2020), https://doi.org/10.1016/j.applthermaleng.2020.115266.

[11] C. Zhao, M. Opolot, P. Keane, J. Wang, M. Liu, F. Bruno, S. Mancin, K. Hooman, Thermal Characteristics of Melting of a Phase Change Material Enhanced by a Stainless-Steel 304 Periodic Structure, Energy Storage Saving. (2023), https://doi.org/10.1016/j.enss.2023.02.002.

[12] M. Opolot, C. Zhao, P.F. Keane, M. Liu, S. Mancin, F. Bruno, K. Hooman, Discharge performance of a high temperature phase change material with low-cost wire mesh, Appl. Therm. Eng. 223 (2023), https://doi.org/10.1016/j.applthermaleng.2023.120050.

[13] M.J. Ganji, M. Givian, K. Gharali, S. Ebadi, S. Maleki Dastjerdi, Experimental optimization of partial metallic wire mesh configuration applicable in thermal energy storage systems, Appl. Therm. Eng. 218 (2023), https://doi.org/10.1016/j.applthermaleng.2022.119274.

[14] C. Zhao, J. Wang, Y. Sun, S. He, K. Hooman, Fin design optimization to enhance PCM melting rate inside a rectangular enclosure, Appl. Energy 321 (2022) 119368, https://doi.org/10.1016/j.apenergy.2022.119368.

[15] A. Pourakabar, A.A. Rabienataj Darzi, Enhancement of phase change rate of PCM in cylindrical thermal energy storage, Appl. Therm. Eng. 150 (2019) 132–142, https://doi.org/10.1016/j.applthermaleng.2019.01.009.

[16] J.M. Mahdi, E.C. Nsofor, Multiple-segment metal foam application in the shell-and-tube PCM thermal energy storage system, J Energy Storage. 20 (2018) 529–541, https://doi.org/10.1016/j.est.2018.09.021.

[17] C. Zhao, M. Opolot, M. Liu, F. Bruno, S. Mancin, K. Hooman, Numerical study of melting performance enhancement for PCM in an annular enclosure with internal-external fins and metal foams, Int. J. Heat Mass Transf. 150 (2020), https://doi.org/10.1016/j.ijheatmasstransfer.2020.119348.

[18] C. Ao, S. Yan, W. Hu, L. Zhao, Y. Wu, Heat transfer analysis of a PCM in shell-and-tube thermal energy storage unit with different V-shaped fin structures, Appl. Therm. Eng. 216 (2022), https://doi.org/10.1016/j.applthermaleng.2022.119079.

[19] J. Li, Z.R. Abdulghani, M.N. Alghamdi, K. Sharma, H. Niyas, H. Moria, A. Arsalanloo, Effect of twisted fins on the melting performance of PCM in a latent heat thermal energy storage system in vertical and horizontal orientations: Energy and exergy analysis, Appl. Therm. Eng. 219 (2023), https://doi.org/10.1016/j.applthermaleng.2022.119489.

[20] G. Righetti, C. Zilio, G.A. Longo, K. Hooman, S. Mancin, Experimental study on the effect of metal foams pore size in a phase change material based thermal energy storage tube, Appl. Therm. Eng. 217 (2022), https://doi.org/10.1016/j.applthermaleng.2022.119163.

[21] M. Opolot, C. Zhao, M. Liu, S. Mancin, F. Bruno, K. Hooman, Investigation of the effect of thermal resistance on the performance of phase change materials, Int. J. Therm. Sci. 164 (2021) 106852, https://doi.org/10.1016/j.ijthermalsci.2021.106852.

[22] S. Kline, F. McClintock, Describing Uncertainties in Single-Sample Experiments, Mech. Eng. 75 (1953) 3–8.

[23] S. Mancin, A. Diani, L. Doretti, K. Hooman, L. Rossetto, Experimental analysis of phase change phenomenon of paraffin waxes embedded in copper foams, Int. J. Therm. Sci. 90 (2015) 79–89, https://doi.org/10.1016/j.ijthermalsci.2014.11.023.

[24] S. Zhang, L. Pu, S. Mancin, Z. Ma, L. Xu, Experimental study on heat transfer characteristics of metal foam/paraffin composite PCMs in large cavities: Effects of material types and heating configurations, Appl. Energy 325 (2022) 119790, https://doi.org/10.1016/j.apenergy.2022.119790.